DEPARTMENT OF
ENERGY, MINES AND RESOURCES
MINES BRANCH
OTTAWA

EXPLORATORY STUDY ON GALVANIZING OF IRON SINGLE CRYSTALS

G. E. RUDDLE and J. J. SEBISTY

PHYSICAL METALLURGY DIVISION

MARCH, 1972

Research Report R 247

Price 75 cents

Available by mail from Information Canada, Ottawa,
and at the following Information Canada bookshops:

HALIFAX
1735 Barrington Street

MONTREAL
1182 St. Catherine Street West

OTTAWA
171 Slater Street

TORONTO
221 Yonge Street

WINNIPEG
393 Portage Avenue

VANCOUVER
657 Granville Street

or through your bookseller

Price: 75 cents Catalogue No. M38-1/247

Price subject to change without notice

Information Canada
Ottawa, 1972

Mines Branch Research Report R247

EXPLORATORY STUDY ON GALVANIZING OF IRON SINGLE CRYSTALS

by

G. E. Ruddle* and J. J. Sebisty*

- - - -

ABSTRACT

Single crystals of iron with a range of low-index orientations were galvanized in pure zinc in a specially constructed hydrogen atmosphere apparatus.

Significant reaction effects found on (110), (100), and (111) surfaces of commercial single crystals indicated a positive relationship between galvanizing reactivity and crystallographic orientation of the iron substrate surface. The nucleation and growth mode of the predominant ζ iron-zinc alloy layer in the coatings was presumably affected thereby.

Differences in reaction behaviour which remain to be explained were found with the commercial crystals and strain-annealed enamelling-iron crystals of the same orientation.

Normal reaction effects were found on enamelling-iron crystals with other orientations such as (421), (311), (210), and (221).

---

* Research Scientist, Non-Ferrous Metals Section, Physical Metallurgy Division, Mines Branch, Department of Energy, Mines and Resources, Ottawa, Canada.

Direction des mines
Rapport de recherches R 247

Étude de recherches sur la galvanisation des monocristaux de fer

par

G.E. Ruddle* et J.J. Sebisty*

Résumé

On a galvanisé dans du zinc pur des monocristaux de fer avec une gamme d'orientation à indices faibles dans un appareil à atmosphère d'hydrogène spécialement construit pour cet essai.

Les effets de réaction significatifs trouvés sur les surfaces des monocristaux commerciaux (110), (100) et (111) ont indiqué une relation positive entre la réactivité de galvanisation et l'orientation cristallographique de la surface du substrat de fer. Ainsi la germination et la façon de la couche prédominante d'alliage fer-zinc ζ dans les revêtements étaient affectées.

En étudiant les cristaux commerciaux et les cristaux de fer, de même orientation, d'une qualité pour émailler qui sont formés par le procédé de recuit après déformation, les auteurs ont observé des différences de réaction qu'ils ne peuvent encore expliquer.

Les auteurs ont trouvé des effets de réaction normale sur les cristaux de fer d'une qualité pour émailler avec différentes orientations telles que (421), (311), (210) et (221).

---

*Chercheur scientifique, Section des métaux non ferreux, Division de la métallurgie physique, Direction des mines, ministère de l'Énergie, des Mines et des Ressources, Ottawa, Canada.

CONTENTS

INTRODUCTION

It is well recognized that the galvanizing reactivity of iron, or steel, is largely dependent on the chemical and physical nature of the substrate material. More precisely, the parameters which can significantly alter the reaction rate include the chemical composition, degree of strain, grain size and surface topography of the substrate. The influence of these factors has been extensively studied, usually, it might be added, in terms of the properties as they apply to the bulk material. On the other hand, little or no attention has been paid to the crystallographic characteristics of the surface. This aspect would appear to have particular relevance when it is considered that only the outermost few microns of the iron or steel surface take part in the reaction.

As a step in this direction, an exploratory investigation was undertaken to study the effects of crystallographic orientation of the iron substrate on galvanizing reaction kinetics. It was of primary interest to establish the possible existence of differences in the rate of zinc attack on surfaces of different crystallographic orientation. Extrapolation of the results to the textured surface of polycrystalline steel sheet and strip, if warranted and feasible, presented the possibility of developing improvements in galvanized-coating techniques and properties. The investigation involved galvanizing experiments in a specially built hydrogen atmosphere apparatus in which single crystals of iron of different orientation and purity were coated in unalloyed zinc baths over a range of time-temperature conditions. The investigation was performed with the co-operation and support of the Canadian Zinc and Lead Research Committee and, in part, of the International Lead Zinc Research Organization, Inc.

EXPERIMENTAL PROCEDURE

Apparatus

The experimental galvanizing method, initially considered, was a thermobalance technique in which iron-zinc reaction effects could be examined by continuous monitoring of the weight change of immersed single crystal samples. This idea was rejected because of major experimental difficulties to be expected in interpretation and evaluation of the precise weight changes involved [1]. An alternative batch system was adopted which provides for reacting hydrogen-reduced iron and steel sheet in a bath of filtered zinc maintained in a hydrogen atmosphere. Sample immersion through a clean mirror-bright surface and elimination of conventional pickling and fluxing pretreatments are principal features of the method. A schematic layout and a photograph of the apparatus are shown in Figures 1 and 2.

The reaction chamber is a water-cooled stainless steel tube 8 in. (20 cm) in diameter and 36 in. (90 cm) long which can be evacuated to 2μ by a two-stage mechanical pump. The chamber houses two furnace units with appropriate radiation shielding to reduce temperature gradients. Hydrogen reduction of surface oxides on the suspended samples is done in the upper unit at a sample temperature of 450°C (840°F). In operation, a continuous metered flow of purified hydrogen is maintained through the hollow push rod to provide a flushing circulation near the bath surface. The system as a whole is maintained at a slight positive pressure. Hydrogen purification is achieved with a commercial diffusion unit operating at a pressure of 250 psi (1.7×10^6 N/m^2) and a temperature of 275°C (525°F). The purification is based on the high permeability of hydrogen isotopes through a 75% Pd-25% Ag alloy. Nitrogen, oxygen, carbon monoxide, hydrocarbons, and water vapor present in commercial hydrogen are thereby excluded. The unit installed has a capacity of 5 cu ft/hr (150 ℓ/hr).

A pre-cast 3-lb (1.4-kg) machined charge of zinc is melted and filtered in the high-purity graphite double-crucible assembly shown in Figure 1. Melting is done in the lower crucible, and the zinc is transferred into the movable upper crucible through fine holes in a graphite disc, in series with a pad of silica wool. The close-fitting upper crucible is forced down by manual operation of the filtering pressure rod. This technique to obtain an oxide-free melt was selected in preference to hydrogen reduction for various reasons. Principally, recent evidence [2] has shown that the kinetics of hydrogen reduction of zinc oxide are very slow around 450°C (840°F). More intimate contact of the reactants by bubbling of the melt increases the reaction rate but, from trials made, this method was discarded because of excessive apparatus contamination by spattering and volatilization of zinc.

A complete experimental cycle is a two-day operation. The first is taken up with lengthy vacuum degassing at temperatures around 650°C (1200°F). This is unavoidable because of the contained refractory components and is also necessary for de-zincing of the graphite crucible assemblies so they can be re-used. Evacuation to about 5μ can be achieved after several hours and the chamber is then filled with high-purity nitrogen and left to cool overnight. This minimizes water vapor absorption during the short time the chamber is re-opened for charging.

After re-opening, any zinc condensate deposited during degassing is removed, the zinc charge and samples are loaded, and the filtering unit is assembled. After sealing and evacuation to about 25μ, the chamber is filled with hydrogen for an initial sample-reduction treatment of 45 min at 450°C (840°F). The measured temperature at the zinc charge is of the order of 25°C (75°F) and zinc volatilization is therefore negligible. To remove the products of the reduction reaction, the chamber is again evacuated and, at the same time, further degassing of the melt furnace assembly is achieved by heating to 100°C (210°F) for 1 hr. Evacuation is continued to below 5μ.

After refilling with hydrogen, both furnaces are activated and during melt-down a second sample-reduction treatment is applied for 1 hr at 450°C (840°F). The filtering operation follows, and, while the bath temperature is restabilized, the bath surface is visually monitored for cleanliness. The samples are manually lowered and immersed for galvanizing and then withdrawn for cooling to the central zone of the chamber. The temperature in this zone does not exceed 175°C (345°F) by the time the withdrawal of samples is initiated. After shut down, the hydrogen-filled chamber is left sealed overnight for cooling.

More complete descriptions of the apparatus and of the problems involved in bringing it to an acceptable operational status are to be found elsewhere [3, 4]. The principal difficulty was related to re-formation of oxide on the zinc melt which was always mirror bright immediately after filtering. This was attributed to the presence of water vapor in the reaction chamber atmosphere. The nature of the problem may be appreciated from the fact that at 450°C (840°F), only 1 ppm of water vapor is thermodynamically necessary for initiation of the reaction with zinc to form zinc oxide. The thermodynamic prediction is considered to be reasonable because the activation energy for the oxidation of liquid zinc is expected to be relatively small.

The sources of water vapor would be (i) residual molecules in the chamber vacuum, and adsorbed molecules on the refractory components and other surfaces within the chamber, (ii) molecules introduced by movement of the filtering rod and the sample support rods through the seals in the top of the chamber, and (iii) molecules produced in the hydrogen reduction of oxides on the sample surfaces. These sources are inherent in the reaction apparatus design and operation. Thus, the concentration of residual water vapor present could be expected to be more than adequate to initiate and sustain some degree of melt oxidation. The success in reducing this to a minimum, as exemplified by the ingot in Figure 3, is therefore particularly noteworthy. The surface contamination usually took the form of isolated agglomerates of small particles surrounded by clean metal. The individual particles could be resolved at low magnifications. Analyses by high-energy electron diffraction (HEED) and spark emission mass spectroscopy on the particles (Analytical Chemistry Section, Metallic Corrosion Section, Chemistry Division, National Research Council, Ottawa) revealed the presence of a high concentration of oxygen in the form of various metal oxides, primarily zinc oxide (4).

Iron Single Crystals

(a) Materials

Commercial single crystals of iron equivalent in purity to Armco iron were obtained for the principal part of the investigation. These are designated as Cambridge crystals: 8° off (100) and 7° off (110) and as Cleveland crystals:

up to 7° off (111). They were intended to represent three of the basic low-index-plane orientations in the body-centred cubic structure of alpha iron.

Single-crystal grains cut from strain-annealed enamelling-grade iron sheet were used in preliminary tests as well as in the main series of galvanizing experiments. The orientations selected were similar to the commercial crystals,and also represented the mid-point and mid-sides of the basic stereographic triangle. These were laboratory produced by isothermal strain-annealing of strips of enamelling iron 6 x 0.50 x 0.05 in. (152 x 13 x 1.3 mm) which were reduced by 30% to 0.035 in. (0.9 mm), vacuum annealed for 3 hr at 830°C (1525°F), tensile strained to 5%, and vacuum annealed for 72 hr at 890°C (1635°F). Surface contamination was minimized between the different stages by chemical polishing for 10 sec in a solution of 80% H_2O_2, 5% HF, and 15% H_2O. The grain structure of the strain-annealed iron samples was revealed by immersion for 10 sec in an etchant of 25% HNO_3 in water.

The crystallographic orientations of several large grains in each of the strain-annealed samples were determined by Laue back-reflection X-ray diffraction [5] to enable the selection of the desired orientations. The X-ray diffractions were made with Co target radiation generated at 40 kV and 10 mA. Surface orientations suitable for the investigation were found in all low-index orientations except in the (100) region. The surface orientations of the commercial crystals were also confirmed by the same technique. Suppliers' analyses for the commercial crystals,and quantometer analyses (Spectrochemistry Section, Mineral Sciences Division, Mines Branch, Ottawa) made on the enamelling-iron stock sheet, are given in Table 1. The presence of a significant amount of silicon (0.019%) in both Cambridge commercial crystals was confirmed by DC arc spectrography (Analytical Chemistry Section, Chemistry Division, National Research Council, Ottawa).

(b) Pretreatment

The Cambridge crystals were supplied as flat strips 2 to 3 in. (50 to 75 mm) long, 0.5 in. (13 mm) wide and 0.04 to 0.06 in. (1 to 1.5 mm) thick. These were cut into samples 0.5 in. (13 mm) long and suspension holes were bored by the strain-free technique of spark machining. Each crystal was cemented to a supporting electrode with a mixture of glyptal cement and graphite powder and additional electrical contact was provided with Fullam Silver Print. The cutting electrodes were made from thin-gauge copper sheet or wire appropriate for producing straight cuts and holes, respectively. After spark-cutting, the cements were dissolved away with acetone. Swabbing and ultrasonic washing in acetone or iso-amyl acetate was necessary to remove residual silver print. The Cleveland crystals were supplied as round discs 0.375 in. (10 mm) in diameter and from 0.08 to 0.1 in. (1 to 2.5 mm) thick.

Suspension holes were bored by drilling. In the case of the strain-annealed enamelling iron, polygon-shaped single crystals with selected orientations in sizes equivalent to 0.25 in.^{2} (160 mm^2) or less were cut out with a jeweller's saw. Suspension holes were also drilled in these crystals.

A flat, smoothly polished, strain-free surface was desired for study of the orientation effect on the galvanizing reaction. It was initially necessary to eliminate etch-pitting irregularities on all the crystal samples by mechanical grinding. The procedure involved flush mounting of the crystal by Pellon "KK" double-faced adhesive onto a brass supporting disc, curing of the adhesive at 80°C (175°F) for 0.5 hr, grinding the crystal by dry lapping on 400 grit silicon carbide paper until the etch pits were removed, and then successive lappings of the crystal on 600 grit and 600 soft papers. Finally, the adhesive was softened by heating to permit separation of the crystal from the brass supporting disc and then dissolved from the crystal in methyl ethyl ketone. Both surfaces of each crystal sample were similarly treated.

Surface levelling was followed by polishing treatments to remove the deformation layer resulting from mechanical grinding. On the basis of trials with enamelling iron, a procedure was adopted combining chemical polishing (6) to maintain surface levelling and a short-time electropolish (7, 8) to produce a final polish of maximum smoothness. Details are given in Appendix A. At least 0.002 in. (0.05 mm) was removed in total to provide crystal surfaces which were indicated by X-ray diffraction and microscopic examination to be essentially free of deformation.

The final pre-treatment step was an integral part of the galvanizing operation and entailed reduction of the iron surface in a purified hydrogen atmosphere. This removed any surface oxide formed anodically in final polishing and atmospherically after polishing, thus producing an oxide-free iron surface for galvanizing.

Surface examinations were made of the (100) and (110) surfaces of the Cambridge iron crystals, before and after reduction in the hydrogen apparatus. The purpose was to determine the effect of the reduction treatment on the polished surface and the possible existence of a correlation between the topography of the single crystal surface and the galvanizing response. In an initial attempt by scanning electron microscopy, no surface features characteristic of the crystallographic orientation could be resolved. The crystal surfaces were subsequently examined by the higher-resolution technique of replica electron microscopy. Replicas of the surface were made in a two-stage process. In the first, a replica of plastic (Biodene) was formed on the crystal surface and the plastic was shadowed in vacuum with chromium at an angle of 25°. In the second, a replica of carbon was vacuum-deposited over the shadowed plastic. The double replica was mounted on a 200-mesh support grid and the plastic was dissolved away in acetone leaving

the chromium-shadowed carbon replica on the grid for examination by electron microscopy.

Galvanizing Experiments

All galvanizing experiments were done in the hydrogen atmosphere apparatus described in a previous section. Operations of reduction of the iron surfaces, melting and filtering of the zinc bath, and immersion of the crystal samples in the zinc bath, all in a purified-hydrogen atmosphere, were integrated in each experiment. The conventional pre-treatments of pickling and fluxing were thereby eliminated and samples with clean oxide-free surfaces were immersed into the filtered bath through a clean bath surface.

The experiments completed are listed in Table 2. These covered the commercial crystals with surface orientations near (100), near (110), and near (111) and the enamelling-iron crystals of selected low-index surface orientations representing the (110) and (111) corner points, a centre point, and mid-points of the sides of the stereographic triangle (Figures 4, 5 and 6). From preliminary experiments, it was indicated that relatively short immersion times were required for detection of an orientation effect and the following were selected: 15 sec, 1, and 2.5 min. All experiments were run in special high-grade (99.99%) zinc at a bath temperature of 452 $\pm$ 2°C (840 $\pm$ 4°F). Pairs of crystal samples suspended one above the other were galvanized for each immersion time. Galvanizing of three pairs of the crystals was repeated at 500°C (930°F) for 5 min to compare the orientation effect in or near the temperature range for linear galvanizing kinetics.

Evaluation of the galvanizing behaviour of the crystals was made by metallographic examination of one of each pair of samples and by measurement of iron weight loss on the other. Sections for metallography were cut out with a jeweller's saw such that the remainder of the crystal samples could be stripped of their coatings and re-used. Each small section was mounted in a clip, custom-formed from galvanized steel sheet. The clip provided (i) retention of the crystal section during vacuum impregnation with epoxy resin and during pressing into the diallylphthlate mount, and (ii) protection of the coating edges during metallographic polishing. The galvanized coating on the clip also provided the appropriate galvanic action in the chemical etching of the coating structure. Established techniques of metallographic polishing and etching were used. The crystals for the measurement of iron weight loss were weighed before galvanizing, stripped after galvanizing in a 1:5 solution of HCl and H_2O, weighed, and measured for surface area to determine the weight loss per unit of surface area. As discussed in the next section, the results were not consistent with metallographic observations in several cases; iron loss values based on measurements of iron-zinc alloy thickness are reported instead for the complete range of experiments.

RESULTS

Iron Weight Loss Measurements

The iron weight loss w in the galvanizing reaction has been expressed as a function of immersion time t in the general kinetic relation

$$w = ct^m$$

where c is a proportionality constant and the exponent m characterizes the reaction kinetics. On the premise that iron is consumed according to this relation, the rate constants c and m may be determined by graphical analysis of a log-log plot of iron weight loss (g/m^2) as a function of immersion time (sec).

Correlation of the iron weight losses (as determined by normal chemical stripping procedures) and the coating microstructures revealed more inconsistencies with the Cleveland and enamelling-iron crystals than with the Cambridge material. The iron loss discrepancies were presumably related in some degree to the following: (i) edge surfaces of the crystal samples represented from 10 to 35% of the total surface area, hence any differences in reactivity associated with edge surfaces and corners would be proportionately significant, (ii) errors in measurement of the relatively small surface areas and small weight losses , (iii) possible minor attack by the stripping reagent on sample areas more thinly coated because of zinc drag-out effects, and (iv) differences in reaction behaviour at sites of small tramp grains which are inherent in production of iron single crystals. It may be noted that the samples in each run (Table 2) were immersed in fresh zinc within a short time of each other. Iron contamination of the bath could therefore not have influenced the iron loss measurements. This effect would have been minimized in any event because of the small size of the samples relative to the bath volume.

Alternative iron loss values were calculated from the average iron-zinc alloy thickness as measured on representative microsections. An average density of 7.18 g/cc and an average iron content of 7% for the alloy layers as a whole was assumed. As illustrated and discussed later, alloy growth was frequently of uniform thickness, and reliable measurements were possible. The results obtained are graphically presented on logarithmic co-ordinates in Figures 4-6. It should be noted in the discussion to follow that "reactivity" is indicated by the magnitude of the iron weight loss at a particular immersion time, whereas "reaction rate" is represented by the slope m of the iron weight loss versus immersion time curve.

Figure 4 shows that the enamelling-iron orientations at the centre and mid-sides of the basic stereographic triangle and enamelling-iron polycrystals behaved similarly as a group. Low galvanizing reactivity was indicated and, in every case, the surfaces reacted at equally low rates well below the parabolic value of 0.5. Essentially the same reaction rate is shown in Figure 5 by the enamelling iron (110) and (111) orientations, although the latter exhibited a higher weight loss at all immersion times.

The comparison of Figures 5 and 6 reveals major differences between the enamelling-iron and the commercial crystals. For example, with the (111) orientations, reactivity of the Cleveland crystals was markedly lower than the enamelling iron. At the same time, a higher reaction rate with the Cleveland crystals was well defined so that with longer immersion times the two weight loss curves would eventually cross. More striking was the pronounced difference between the (110) crystal surfaces. The very high reactivity and reaction rate on the Cambridge (110) samples in Figure 6 clearly bears no relation to the response of the corresponding enamelling-iron orientation in Figure 5. Although the Cambridge (110) reaction constant significantly exceeded the value of 0.5 for parabolic kinetics, the results for this orientation are considered to be real for reasons discussed later.

Enamelling iron crystals in the (100) orientation could not be produced by strain annealing and only the single set of iron loss data obtained with the Cambridge (100) crystals is available (Figure 6). It can be seen that the behaviour was intermediate between the high-reactivity Cambridge (110) and low-reactivity Cleveland (111) orientations. Of the seven crystallographic orientations tested this was the single example of iron attack taking place according to a parabolic rate law ($m = 0.5$).

Metallographic Observations

Photomicrographs of transverse sections of the experimental coatings are illustrated in Figures 7-13. Five of the six enamelling-iron orientations, comprising the (110), (421), (221), (311) and (210) surfaces, and the Cleveland (111) surface exhibited coating microstructures similar to that on a polycrystalline enamelling-iron sample subjected to the same surface preparation and galvanizing conditions. Representative microstructures are shown for the polycrystalline sample and (110) surface of enamelling iron in Figures 7(a) and (b) and for the Cleveland (111) surface in Figure 8(c). (The average grain diameter in the polycrystalline material was approximately 0.1 mm). The iron-zinc alloy layers formed were generally uniform and compact, consisting of a thin δ_1 layer and a proportionately thicker ζ layer for the shorter immersion periods. As the immersion time was increased, the layers remained compact and the proportions of the δ_1 and ζ reflected the characteristic reciprocity in growth associated with these phases. The ζ

crystallites adjoining the outer zinc layer were usually rounded off as is typical with a low-iron bath. Within this group of crystal orientations, only on the Cleveland (111) surface was there distinct evidence of a continuous Γ layer.

Entirely different coating microstructures were observed on the remaining three surfaces, namely, the enamelling iron (111), and the Cambridge (110) and (100) orientations. Figures 7(c) and 8(a) and (b) show that the iron-zinc alloy in the coatings consisted almost wholly of compact ζ. The growth rate of this layer was least on the enamelling iron and much more pronounced on the Cambridge crystals, particularly on the (110) orientation. It will be noted that the type of coating microstructure on this latter group, viz., the thick compact ζ layer, very thin δ_1 layer, and absence of Γ is very similar to that commonly found on semi-killed steels containing about 0.10% Si. In the present case, it will be recalled that the silicon content of the Cambridge crystals, as supplied, was much lower at 0.019%.

From these results, it appears that the reactivities of the Cambridge crystal surfaces, differing by a factor of about 2 x as shown in Figures 8(a) and (b), are related to crystallographic orientation. This is confirmed in Figure 11 which will be discussed later. However, orientation was obviously not the only responsible parameter. For example, the reactivity of the Cambridge (110) crystals was very much greater than that of enamelling iron of the same orientation (Figures 7(b) and 8(b)). Conversely, the reactivity of the Cleveland (111) crystals was less than that of the corresponding enamelling-iron crystals (Figures 7(c) and 8(c)).

The indicated reaction effects cannot be related to total impurities because the enamelling iron was substantially less pure than either of the commercial crystal materials (Table 1). To what extent segregation of impurities and strain non-uniformity in the crystal materials were responsible for these differences in reactivity is uncertain. In this connection, it may be noted that the enamelling-iron crystals were somewhat more prone to form local areas of wave-like iron-zinc alloy as in Figure 9(a). Fewer and less pronounced irregularities were observed with the Cambridge and Cleveland commercial crystals, as shown in Figure 9(b). Surface inclusions affecting alloy growth (Figure 10) were again more common in the enamelling iron. It was also suspected that variations in surface pretreatment or the galvanizing conditions may have been responsible for the observed reaction differences. However, from Run 90 (Table 2), in which samples of the five orientations in question were identically treated and galvanized together, all the coating microstructures duplicated those found originally.

In the previous section, reference was made to experimental errors which may have contributed to inconsistencies in the direct iron loss measurements attempted. In this connection, the significance of crystal

edge effects is highlighted by the corner microstructure in Figure 11. The pronounced difference in reactivity shown for edge and surface faces is the more noteworthy in this case because the ratio of iron-zinc alloy thickness is practically identical to that for the Cambridge (100) and (110) orientations in Figures 8(a) and (b). A contrasting example which exhibited minimal edge to surface difference in iron-zinc alloy growth is illustrated in Figure 12.

Unlike the pronounced difference in galvanizing reactivity between the (110) orientations of the enamelling-iron and the Cambridge crystals at 450°C (840°F), more nearly identical behaviour was evident at 500°C (930°F) as shown in Figures 13(a) and (b). Also, the Cleveland (111) orientation was only slightly less reactive at this temperature as may be seen in Figure 13(c). In these coating structures, the ζ phase is absent and the instability of the δ_1 phase adjoining the outer zinc layer is manifested by varying degrees of fragmentation of the δ_1 layer. Of particular note is the granular break-up of the Cambridge (110) coating in Figure 13(b). This is unlike the finely divided δ_1 which is characteristic of mild steel behaviour in the linear attack region around 500°C (930°F) and presumably reflects some effect of the crystallographic structure of the substrate material.

Surface Topography of Hydrogen-Reduced Samples

Replicas of the electropolished Cambridge (100) and (110) surfaces revealed topographic features, illustrated in Figures 14(a) and (b), which are believed to be due to the electropolishing treatment [9]. These appeared to be related to crystallographic orientation, as shown by the blistered and grooved features for the (100) and (110) orientations, respectively, and by the change in topography across the tramp grain boundary (Figure 14(a)).

The reduction treatment of the crystals in the purified hydrogen atmosphere at 450°C (840°F) did not significantly alter the surfaces produced by electropolishing. Replicas of the reduced surfaces showed evidence of crystalline carbon, probably graphite crystallites formed by precipitation of carbon at the iron surface during the reduction anneal [9]. In turn, this indicates that any oxide present on the electropolished iron surfaces was effectively removed in the hydrogen pretreatment. It is uncertain to what extent these surface characteristics may have influenced the galvanizing behaviour.

SUMMARY AND DISCUSSION

Within the limitations of the experiments attempted, indications were obtained of an interdependence between galvanizing reactivity and crystallographic orientation of the iron substrate. Principal reaction effects were found on orientations corresponding to the corner points in the basic stereographic

triangle, namely, the (110), (100) and (111) planes. The level of reactivity could be stated to decrease in the orientation order given, at least for immersion times beyond 1 minute. Coincidentally, the atomic spacing on these planes decreases in the same order and, expressed quantitatively, the respective values are 1.72, 1.22 and 0.7×10^{13} atoms/mm^2. However, the relevance of this relationship with respect to the mechanism of the iron-zinc diffusion reaction is of undetermined significance. In contrast to the corner orientations, those representing the centre and mid-sides of the stereographic triangle, namely - (421), (311), (210) and (221) duplicated the galvanizing behaviour of polycrystalline iron of similar purity; no crystallographic orientation effects were apparent.

As noted from comparing the coatings produced on the different materials having the same orientation, there were various inconsistencies in the results which suggest that the relationship between orientation and galvanizing reaction was a secondary effect. However, the differences, observed on the enamelling-iron polycrystalline and (111) surfaces and particularly on the Cambridge (100) and (110) surfaces, leave no doubt that orientation effects were operative. In the case of the Cambridge crystals, other factors which could have been instrumental were presumably non-existent because both crystal materials originated from the same source and were of similar chemical composition. Furthermore, the iron-zinc alloy microstructures on these planes were identically reproduced on equivalent orientations represented by the edge and surface faces of the Cambridge sample in Figure 11. In addition, the higher-quality surface finish possible on the Cambridge crystals, as discussed later, is to be noted. This evidence of crystal quality could be expected to be reflected in more uniform and reproducible galvanizing reactivity.

The observed behaviour of the enamelling-iron and Cleveland group of crystals, on the other hand, could be considered suspect to some degree. The similar coating microstructures on all except the enamelling-iron (111) surface suggests that the effect of crystallographic orientation may have been masked in some way. To what extent physical and chemical homogeneities may have been responsible is unknown. Nevertheless, such inhomogeneity could be assumed because of the lower purity of the enamelling iron and its greater tendency to produce uneven iron-zinc alloy growth as illustrated in Figure 9(a). Another qualitative indication was the greater difficulty of producing a defect-free surface finish in pretreatment of these materials, presumably because of the greater incidence of inclusions and tramp grains.

Common features of the coating microstructures on the reactive Cambridge (100) and (110) surfaces and the enamelling-iron (111) surface at the shortest immersion time was the rapid ζ layer growth and negligible growth of δ_1. This growth behaviour may be taken as an indication that the reaction surface was the ζ - δ_1 interface and that the rate of zinc diffusion through the ζ

layer was sufficient to sustain ζ growth in lieu of further δ_1 growth. The pronounced difference in the rates of ζ growth observed on the (100) and (110) surfaces of the Cambridge crystals is interpreted to be the result of a difference in rates of inward diffusion of zinc through the ζ layers.

It is presumed that the ease with which the zinc diffused inward through the ζ layer was principally related to the characteristics of the intergranular boundaries in the layer. The ζ phase has been reported as the first alloy layer to be formed in the iron-zinc reaction [10-12]. This being the case and the Cambridge crystals being apparently identical in every respect except orientation, the growth structure of the ζ layer may have been directly influenced by the crystallographic orientation of the iron substrate. The observed difference in rates of ζ growth suggests a modification in ζ-layer structure resulting from the way growth was initiated crystallographically on the iron surface. Any factor affecting the continuity and alignment of intergranular paths formed in the growth of the ζ layer would be expected to have a pronounced effect on the diffusion of zinc. Further investigation by metallographic and electron-diffraction analyses would be necessary to determine textural differences in the ζ layer relative to the iron substrate crystallography.

In the reactions on the Cambridge (100) and (110) surfaces, the evidence that equally thin δ_1 layers were formed and remained at constant thickness throughout the immersion period also suggests that iron was consumed in the reaction by a uniform transformation to δ_1 at the iron-δ_1 interface and by transformation of δ_1 to ζ at the δ_1-ζ (reaction) interface. There is no indication that iron diffusion was by a structure-sensitive mechanism and a relationship between substrate orientation and outward diffusivity of iron to the reaction interface is therefore discounted.

The absence of a substrate-orientation effect generally observed with the enamelling-iron and Cleveland (111) surfaces is not understood. For reasons which are not clear, growth of the ζ phase was initiated in such a way that an apparently more compact layer was formed. The corresponding lower rate of zinc diffusion to the ζ-δ_1 interface would be expected to result in ζ and δ_1 growth rates which would be lower and higher, respectively, than observed on the more reactive surfaces. Consistent with this hypothesis is the reciprocity relation in the proportions of ζ and δ_1 found in regions on the reactive surfaces where ζ growth has been locally suppressed. In Figure 9, it may be noted that the structure of the ζ layer is locally more compact and, presumably, provides a more resistive barrier to zinc diffusion in the regions of suppressed growth than in adjacent regions of freer growth. The structural characteristics of the ζ layer are considered to arise from the way in which ζ growth was initiated on the iron surface and to be perpetuated after the formation of δ_1.

The experimental evidence also suggests that the initial growth form of ζ was not completely dependent on crystallographic orientation of the iron substrate. It appears likely that the chemical and physical quality of the iron may have influenced the sensitivity of ζ growth to crystallographic orientation. Indirect evidence for this was found in the pretreatment operations. With the Cambridge crystals, for example, a more defect-free electropolished surface was attainable; apparently there was a more homogeneous distribution of chemical impurities, particularly inclusions, and lower residual strain in the crystal. These factors and the substantially higher than trace content of silicon (0.019%)may have enhanced the sensitivity of initial ζ growth to the orientation of the iron substrate. The less perfect electropolished surfaces obtained on the enamelling-iron and Cleveland crystals suggested chemically less homogeneous materials with relatively higher residual strains from the strain-annealing process and from prior processing treatments.

The variations in the alloy layer thicknesses as illustrated in Figure 9 may be a result of the influence of inhomogeneities in chemical composition and residual strain in the iron on initial ζ growth. An association between local variations in chemical composition of the iron surface and galvanizing reactivity could possibly be determined in further investigations by electron-probe microanalysis, thereby elucidating the variable reactivity commonly observed in galvanized coatings.

CONCLUSIONS

Enhanced galvanizing reactivity occurred on some crystallographic planes of commercial single crystals of iron. The (110) crystallographic plane was most reactive and the (100) and (111) planes showed decreasing effects in that order. From the characteristicsof the ζ iron-zinc phase which predominated in the coatings on the more reactive surfaces at 450°C (840°F), it appears that the orientation of the substrate affected the nucleation and growth mode of this phase and thereby modified the galvanizing reaction rate and the coating microstructure.

For reasons which remain to be more conclusively established, the same galvanizing response was not reproduced on corresponding crystallographic planes of strain-annealed enamelling-iron crystals.

Enamelling-iron crystals with other orientations such as (421), (311), (210), and (221) exhibited normal galvanizing reactivity similar to that of polycrystalline iron.

REFERENCES

1. Sebisty, J.J. and Brown, W.N. (1968), Physical Metallurgy Division Internal Report PM-R-68-13, Mines Branch, Department of Energy, Mines and Resources, Ottawa.

2. Wright, M.M. and Liang, S.C. (Nov. 1967), private communications .

3. Sebisty, J.J., Brown, W.N. and Palmer, R.H. (1970), Physical Metallurgy Division Internal Reports PM-R-70-2 and PM-R-70-11, Mines Branch, Department of Energy, Mines and Resources, Ottawa.

4. Sebisty, J.J., and Ruddle, G.E. (1971), Physical Metallurgy Division Internal Report PM-R-71-13, Mines Branch, Department of Energy, Mines and Resources, Ottawa.

5. Cullity, B.D. (1956), Elements of X-ray Diffraction, Reading, Mass., Addison-Wesley, pp. 225-229.

6. Marshall, W.A. (1952), J. Electrodepositors Soc. (Trans. Inst. Met. Fin.) 28, 27.

7. Jacquet, P.A. (Nov. 1949), Metal Finishing 47, 62.

8. Tegart, W.J. (1959), The Electrolytic and Chemical Polishing of Metals in Research and Industry, New York, N.Y., Pergamon Press, pp. 50-54.

9. Mitchell, D.F. (Sept. 1971), private communication.

10. Hughes, M.L. (Aug. 1953), Product Finishing 6, 49.

11. Cameron, D.I. (1959), Research Report No. 133, Central Research Laboratory, John Lysaght (Australia) Ltd., Newcastle.

12. Horstmann, D. and Peters, F.-K. (1971), Proc. Ninth International Conf. on Hot Dip Galvanizing (Düsseldorf), London, Industrial Newspapers Ltd., pp. 75-106.

- - - - -

GER/JJS/gm

TABLE 1

Chemical Composition of Iron Crystals

Element (%)	Cambridge Crystals (110),(100)	Cleveland Crystal (111)	Enamelling Iron *
C	.005	.012	<.01
Mn	.03	.017	.295
Si	.03	Trace	<.005
	.019**	<.001**	.014-.016***
P		.005	.010
S		.025	.018
Al			.005
Ni			.038
Cr	.03		.021
Sn			.018
Cu			.040
Mo			.017
Others	<.01		
Fe (by diff)	99.90	99.94	99.5

* Quantometer analyses at surface of stock sheet.

** By DC arc spectrography.

*** Modified quantometer analysis on crystal samples (solution method).

TABLE 2

Galvanizing Experiments

Run and Sample No.	Crystal Sample Data			Galvanizing **	
	Material	Orientation	Pretreatment*	Temp. (°C)	Time (min)
77(2, 3, 1, 4)	Cambridge	8° off (100)	mp, cp(1hr), ep(5 min)	454	$\frac{1}{4}$, 1, 2$\frac{1}{2}$, $\frac{1}{4}$
78(3, 5, 1)	Cambridge	7° off (110)	mp, cp(1hr), ep(5 min)	452	$\frac{1}{4}$, 1, 2$\frac{1}{2}$
(4, 6, 2)	"				
81(4, 3, 1)	Cambridge	8° off (100)	crystals from run 77, cp(1hr), ep (5 min)	450-453	$\frac{1}{4}$, 1, 2$\frac{1}{2}$
82(5, 3, 4)	Cleveland	1-7°off(111)	mp, cp(2$\frac{1}{2}$ hr), ep (12 min)	453	$\frac{1}{4}$, 1, 2$\frac{1}{2}$
(1, 6, 2)	"				
83(2, 4, 6, 8)	Enamelling iron	5° off (110)	mp, cp(1hr), ep (10 min)	451-453	$\frac{1}{4}$, 1, 2$\frac{1}{2}$, $\frac{1}{4}$
(1, 3, 5, 7)	"				
84(2, 4, 6, 8)	Enamelling iron	1-8° off(111)	mp, cp(1hr), ep (10 min)	451-452	$\frac{1}{4}$, 1, 2$\frac{1}{2}$, $\frac{1}{4}$
(1, 3, 5, 7)	"				
85(1, 2, 3)	Enamelling iron	1-3° off (210)	mp, cp(2 hr), ep(8 min)	450	$\frac{1}{4}$, 1, 2$\frac{1}{2}$
(5, 6, 4)	"				
86(1, 3, 4, 2)	Enamelling iron	2° off (221)	mp, cp(2 hr), ep(8 min)	451	$\frac{1}{4}$, 1, 2$\frac{1}{2}$, $\frac{1}{4}$
(5, 6, 7, 8)	"	2° off (421)			
87(3, 2, 1, 4)	Enamelling iron	4-7° off(311)	mp, cp(2 hr), ep(8 min)	450	$\frac{1}{4}$, 1, 2$\frac{1}{2}$, $\frac{1}{4}$
88(4, 2, 1)	Enamelling iron	4-7° off(311)	crystals from run 87, cp(1hr), ep (8 min)	454	$\frac{1}{4}$, 1, 2$\frac{1}{2}$
89(1, 3, 4)	Enamelling iron	2° off (221)	crystals from run 86,	450	$\frac{1}{4}$, 1, 2$\frac{1}{2}$
(5, 6, 7)	"	2° off (421)	cp(1hr), ep(6 min)		
90(2, 1)	Cambridge	8° off (100)	crystals from 5 prior runs,	452	1
(4, 3)	"	7° off (110)	cp(1hr), ep(5 min)		
(8, 7)	Cleveland	4° off (111)			
(6, 5)	Enamelling iron	5° off (110)			
(10, 9)	"	8° off (111)			
91(2, 1)	Cambridge	7° off (110)	crystals from 3 prior runs,	500-502	5
(4, 3)	Cleveland	1° off (111)	cp(1hr), ep (5 min)		
(6, 5)	Enamelling iron	5° off (110)			
92(3, 6, 9)	Enamelling iron	polycrystalline	mp, cp (2 hr), ep(5 min)	452-454	$\frac{1}{4}$, 1, 2$\frac{1}{2}$
(2, 5, 8)	"				

* mp, cp, ep - mechanical, chemical, and electrolytic polish, respectively.
** special high-grade (99.99%) zinc.

A - Hydrogen Inlet

B - Pd / Ag Hydrogen Purifier

C - Sample Holders

D - Filtering Pressure Rod

E - Rotary Seals

F - Stainless Steel Reaction Chamber

G - Water Cooling

H - Hydrogen Outlet

I - Radiation Shielding

J - Reduction Furnace

K - Samples

L - Viewing Ports

M - Metallic Mirrors

N - Graphite Nozzle

O - Pressure Plate

P - Filtering Crucible

Q - Thermocouple

R - Graphite Disc & Silica Wool

S - Melt Furnace

T - Melt

U - Alumina Refractory

V - Liquid Nitrogen Trap

W - To Vacuum Pump

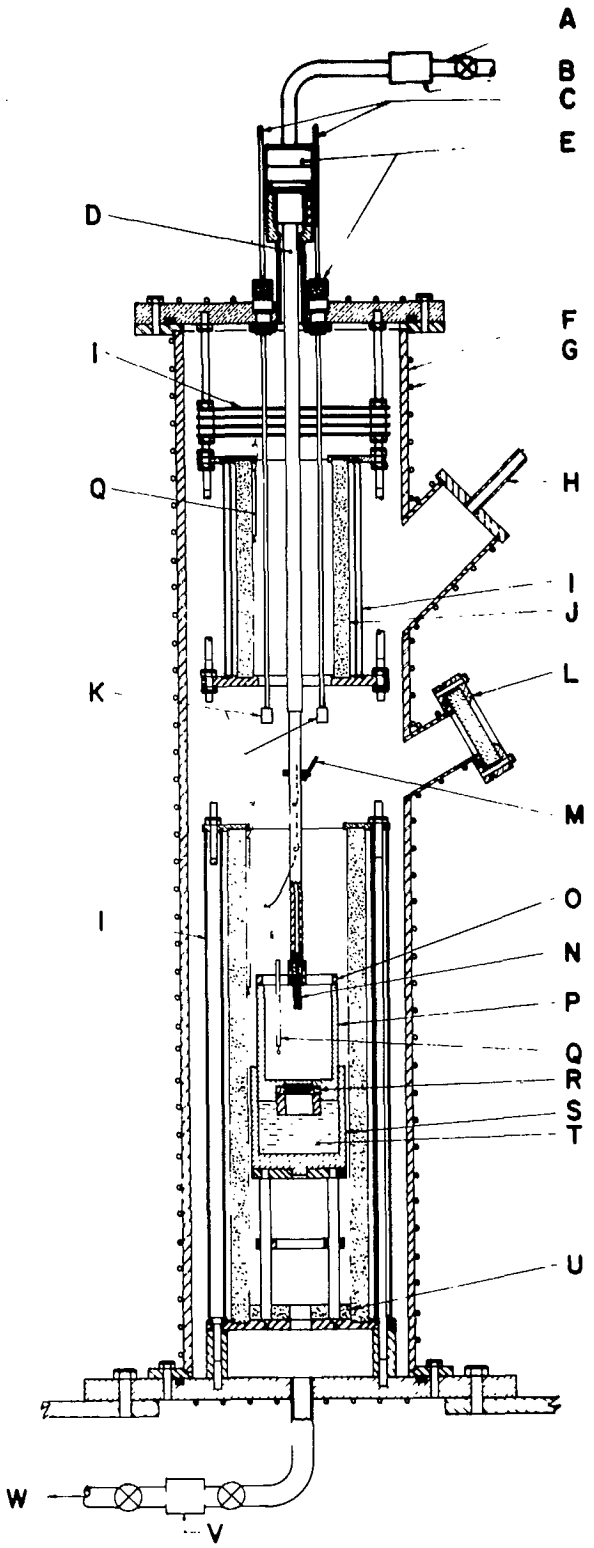

Figure 1. Schematic layout of galvanizing apparatus.

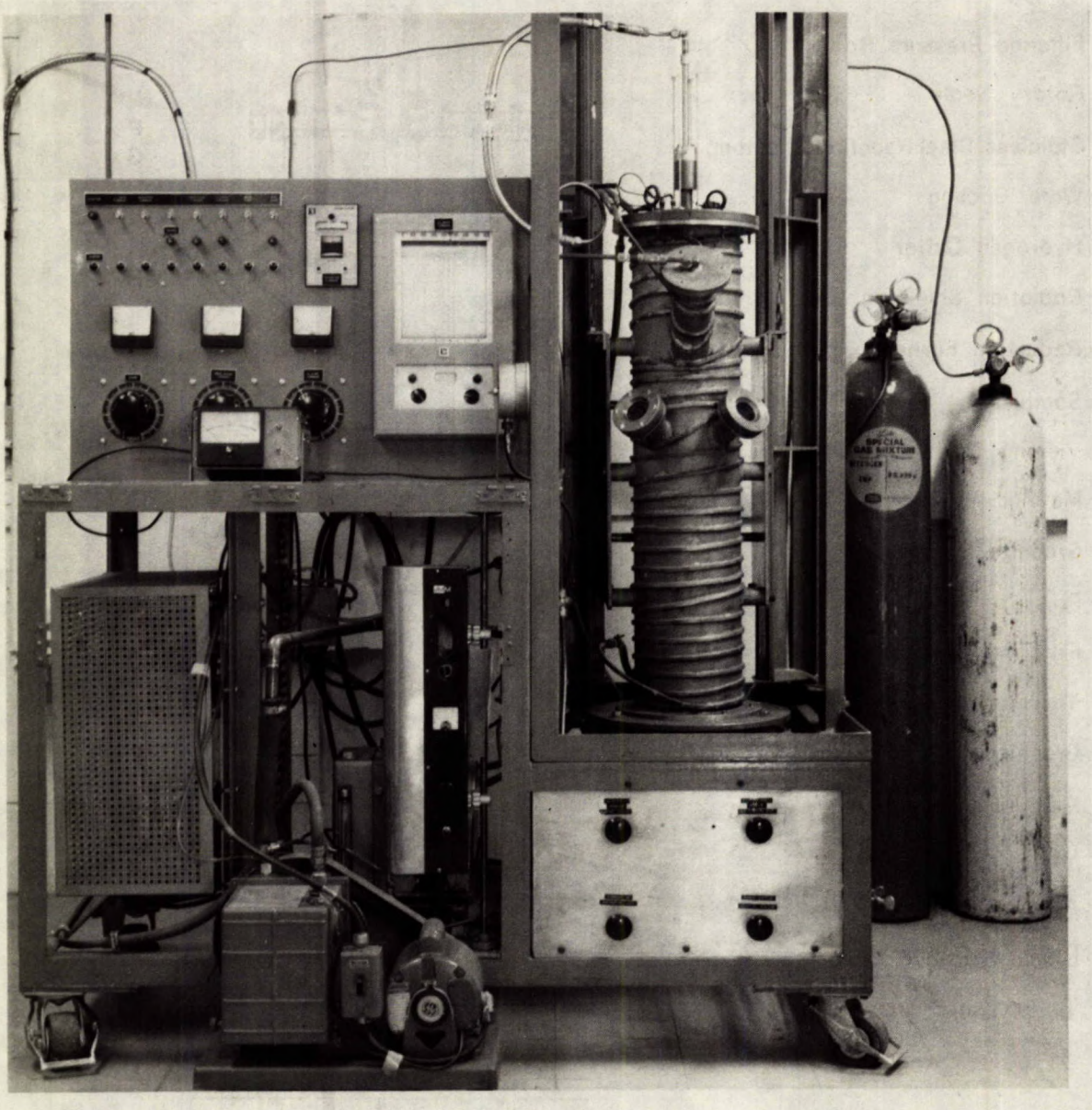

Figure 2. Photograph of galvanizing apparatus.

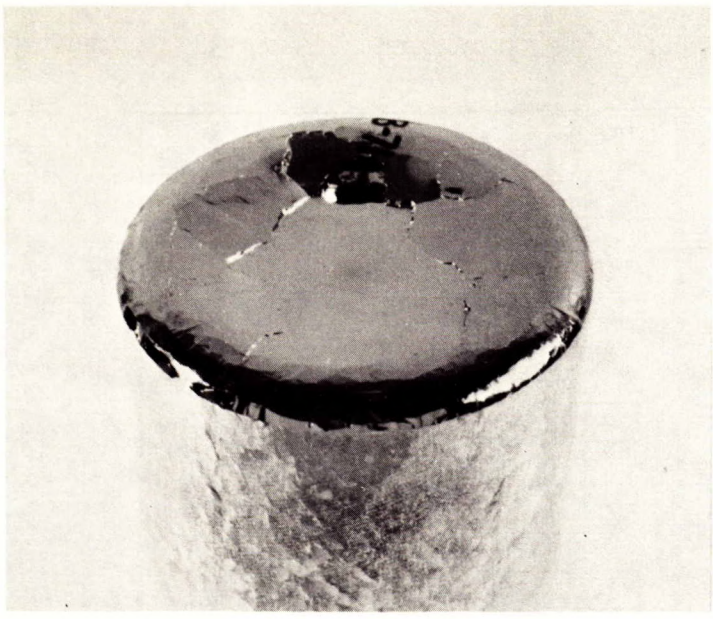

Figure 3. Typical appearance of ingot from experimental filtering run showing large mirror-bright faceted grains.

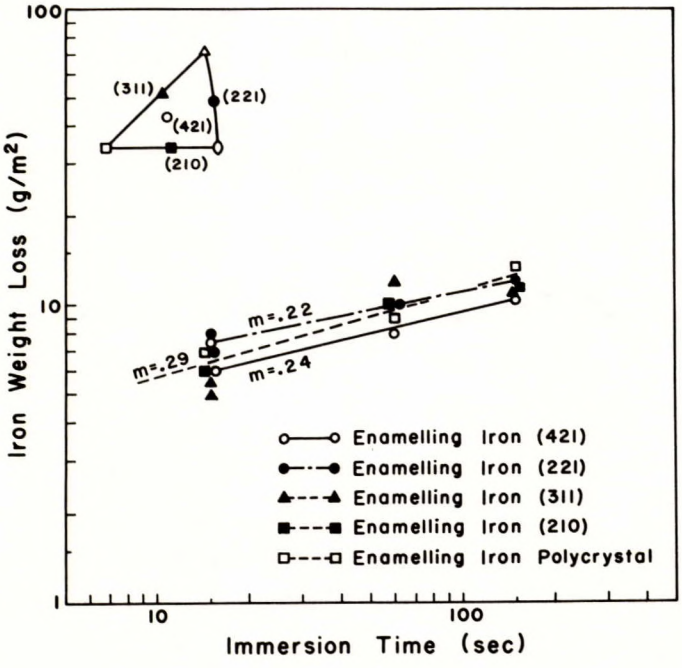

Figure 4. Iron weight loss vs. immersion time for enamelling-iron crystals at orientations indicated.

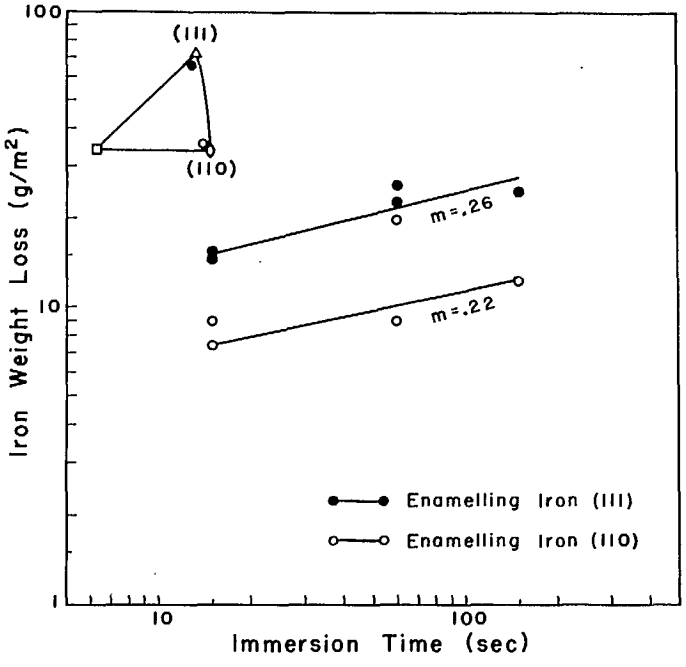

Figure 5. Iron weight loss vs. immersion time for enamelling-iron crystals at orientations indicated.

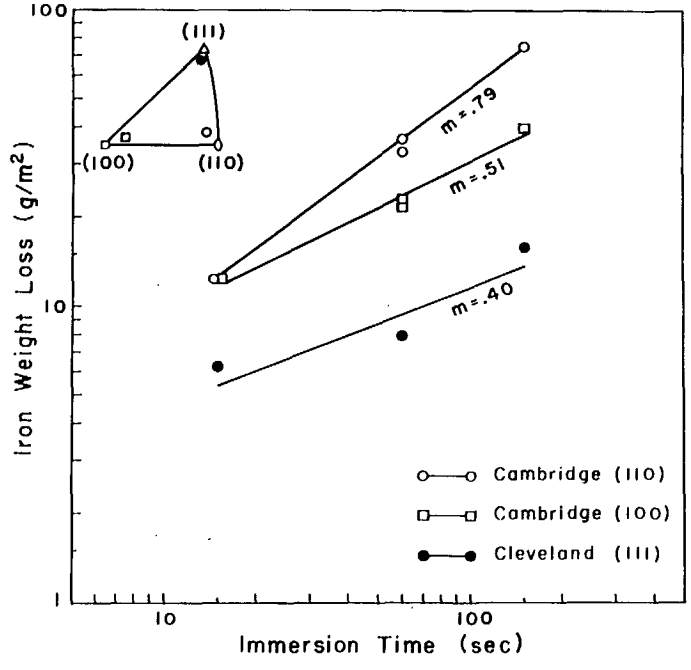

Figure 6. Iron weight loss vs. immersion time for Cleveland (111) and Cambridge (100) and (110) crystals.

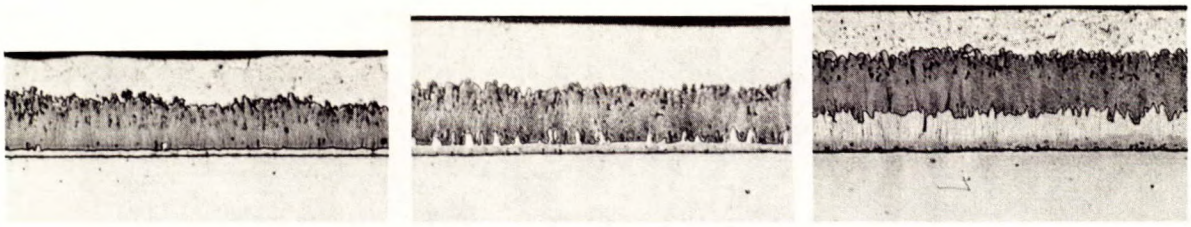

(a) Polycrystalline enamelling iron

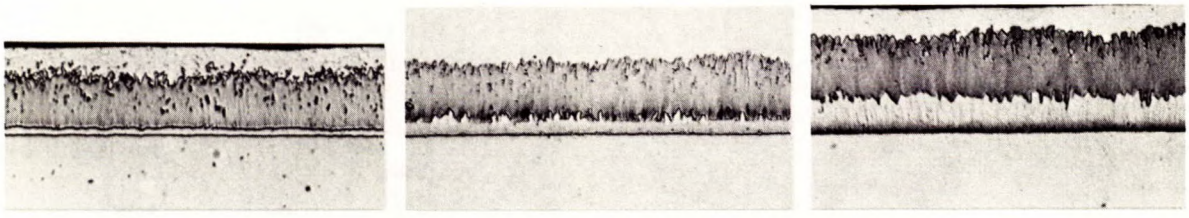

(b) Enamelling-iron (110) surface

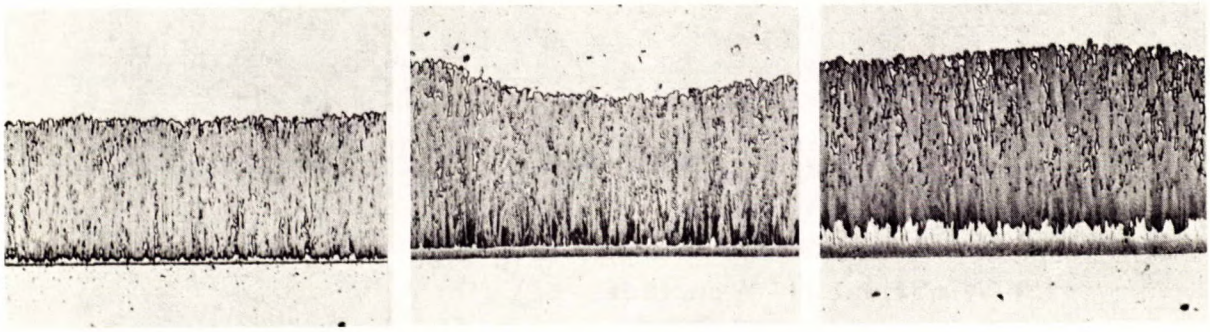

(c) Enamelling-iron (111) surface

15 sec 1.0 min 2.5 min

Figure 7. Coatings on enamelling-iron crystals at 450°C (840°F) for immersion times as shown. X500

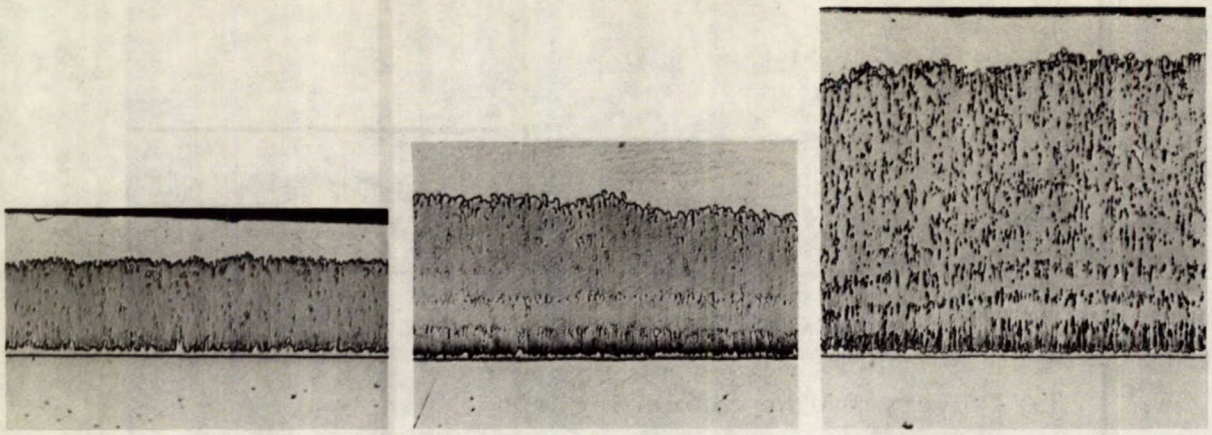

(a) Cambridge (100) surface

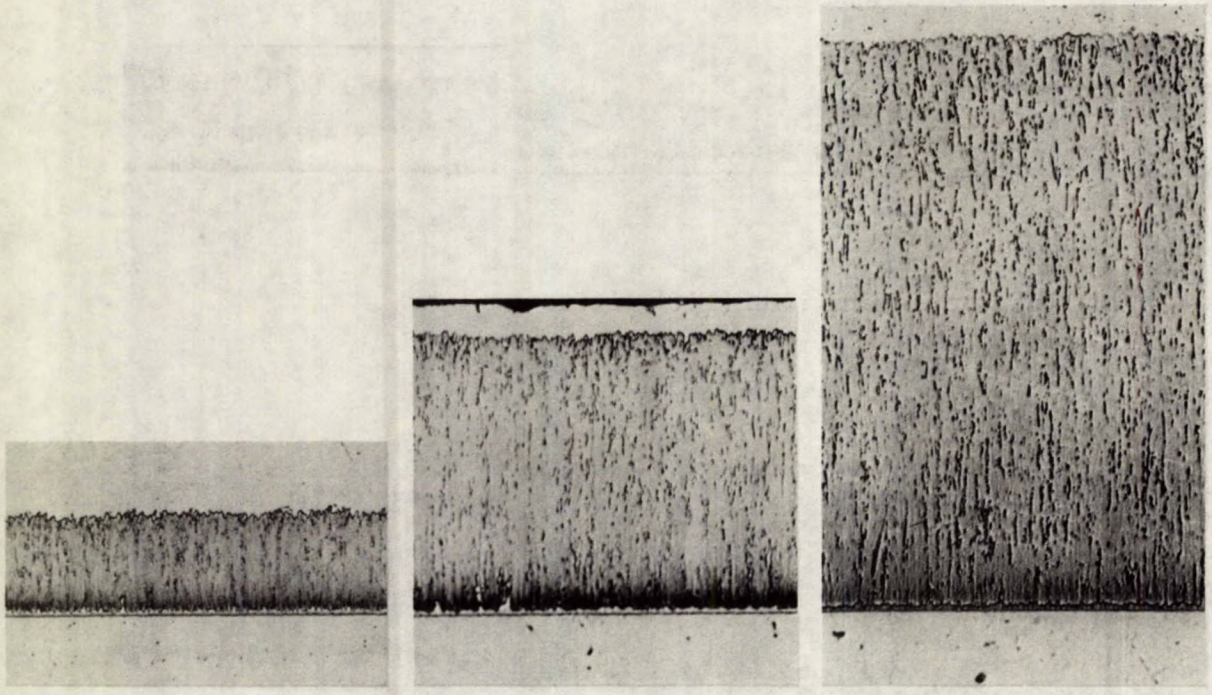

(b) Cambridge (110) surface

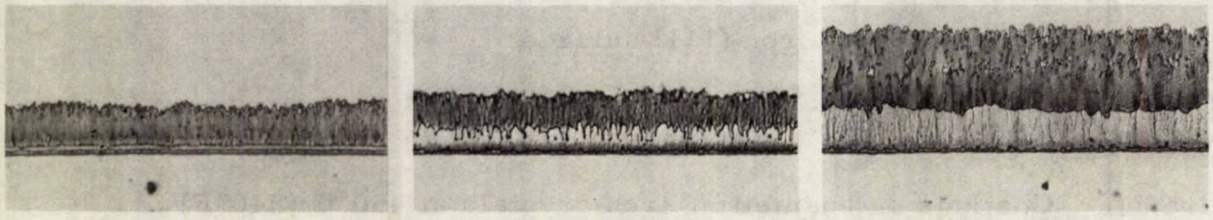

(c) Cleveland (111) surface

15 sec 1.0 min 2.5 min

Figure 8. Coatings on commercial crystals at 450°C (840°F) for immersion times as shown. X500

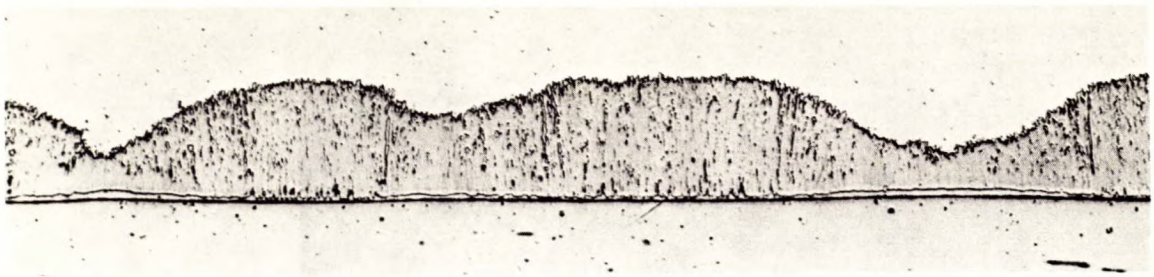

(a) Enamelling iron (111) surface: 15-sec immersion at 450°C(840°F), X500.

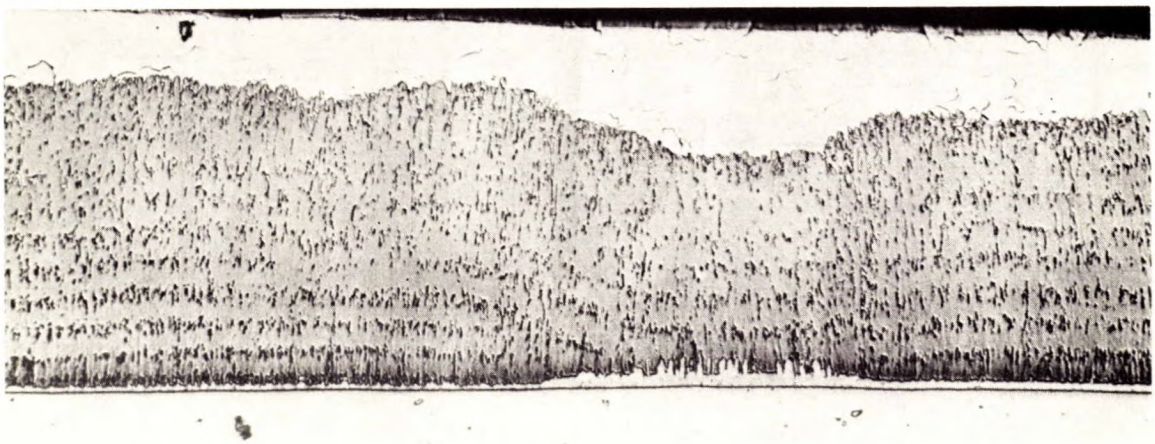

(b) Cambridge (100) surface: 2.5-min immersion at 450°C(840°F), X500.

Figure 9. Coating regions with variations in alloy layer thickness.

Figure 10. Coating regions with localized disruptions in alloy layer resulting from inclusions in enamelling iron: 15-sec immersion at 450°C (840°F), X500.

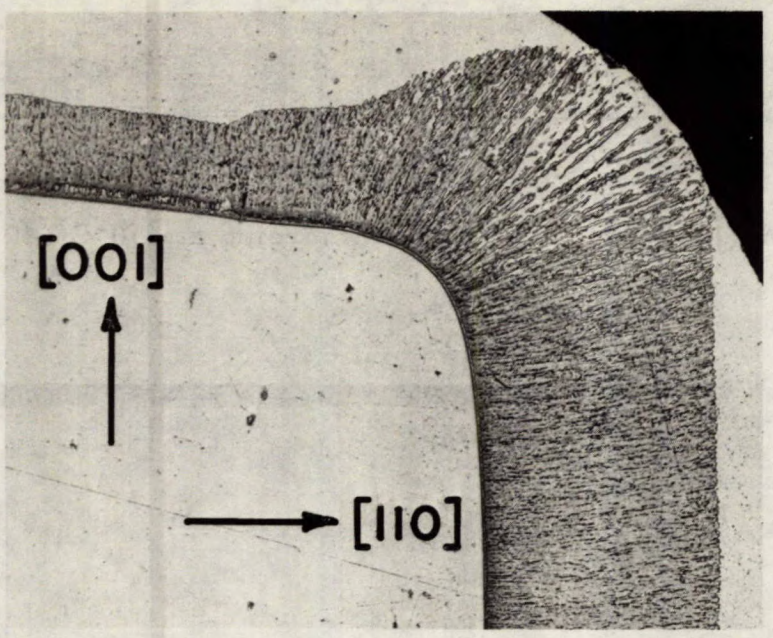

Figure 11. Coatings on edge and face surfaces of Cambridge (110) crystal: 2.5-min immersion at 450°C (840°F), X200.

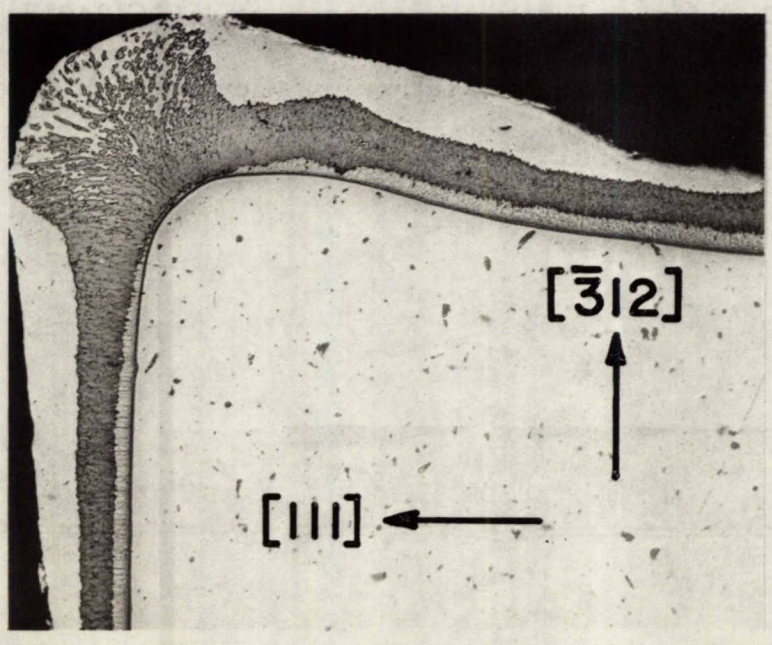

Figure 12. Coatings on edge and face surfaces of Cleveland (111) crystal: 2.5-min immersion at 450°C (840°F), X200.

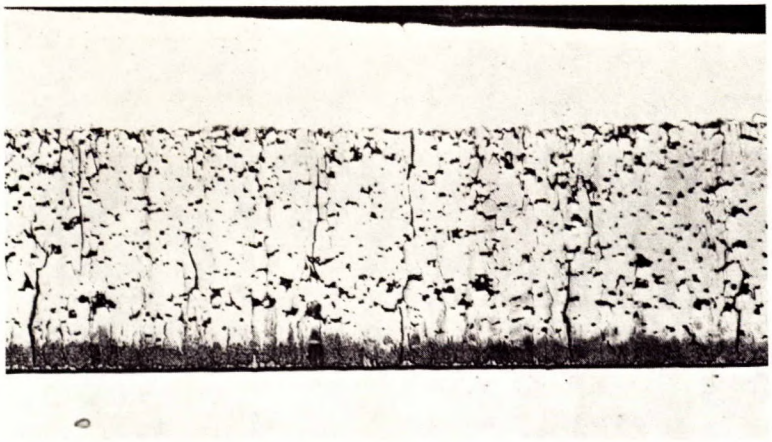

(a) Enamelling-iron (110) surface

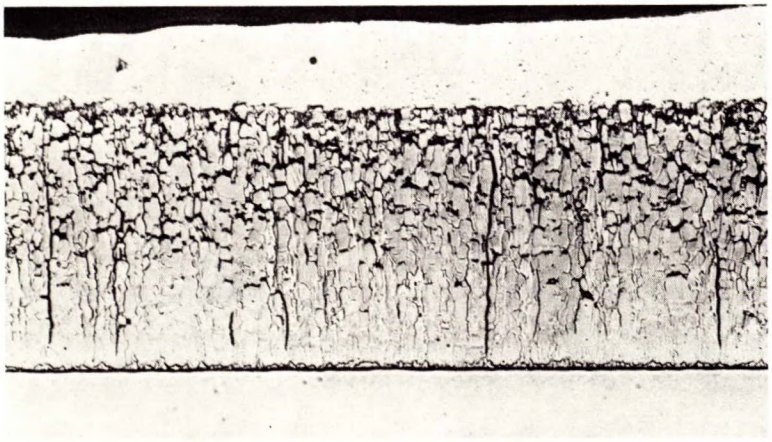

(b) Cambridge (110) surface

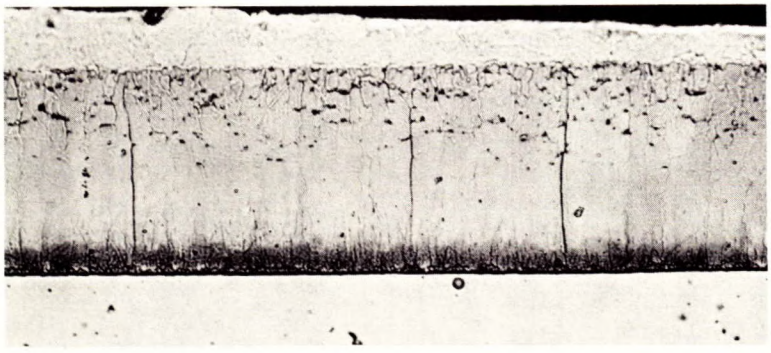

(c) Cleveland (111) surface

Figure 13. Coatings on crystals at 500°C (930°F) for 5 min. X500.

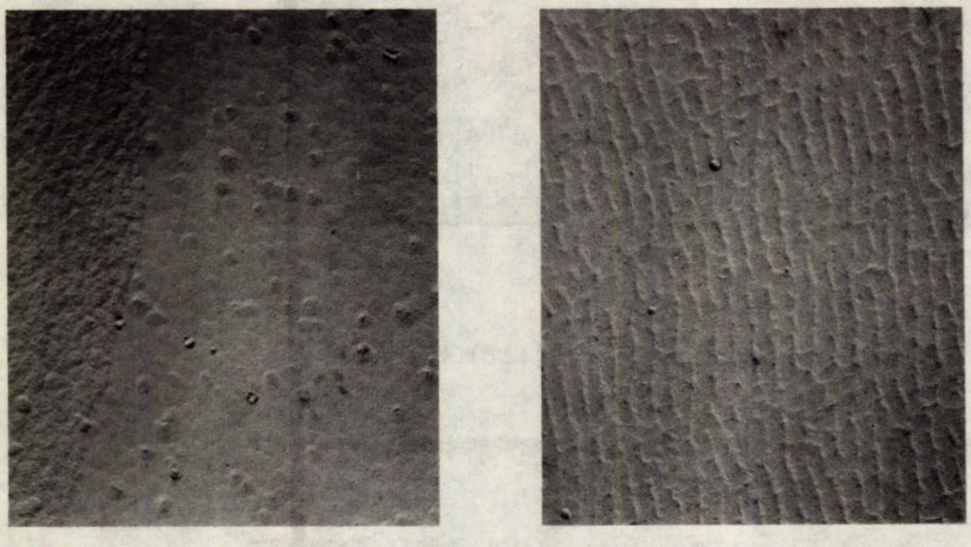

(a) (100) surface with tramp grain on left side.

(b) {110} surface

Figure 14. Surface replicas from electropolished Cambridge crystals. X15,000

APPENDIX A

Chemical Polishing

Marshall's reagent [6] was chosen from a number of recommended chemical polishing solutions because it had the best surface levelling effect. Its relatively strong attack on grain boundaries is no obstacle to polishing single-crystal material. The solution consisted of:

2.5 g oxalic acid (crystals) per 100 ml H_2O
1.3 g hydrogen peroxide per 100 ml H_2O
0.01 g sulphuric acid per 100 ml H_2O

Polishing was carried out at room temperature with no agitation and proceeded at a relatively slow rate requiring a period of one to several hours, depending upon the initial surface roughness. Immediately after removal from the polishing solution, the crystals were given thorough washings, first in distilled water and then in ethanol.

Electrolytic Polishing

A mixture of glacial acetic and perchloric acids has been most generally used for electrolytic polishing of iron. The following procedure was tried and found to produce a satisfactory final polish.

Electrolyte composition:	0.075 vol of 60% perchloric acid to 0.925 vol of glacial acetic acid.

Mixing: add perchloric to glacial acetic slowly with adequate stirring.

Cathodes:	stainless steel plates.
Agitation:	slight magnetic stirring.
Temperature:	cooling water bath to maintain electrolyte temperature at 15 to 28°C (60 to 80°F).
Electrode voltage:	28 V.
Current density:	approximately 40 A/dm^2.
Polishing time:	2 to 5 min.

Washing:	immediately after removal from electrolyte, the sample is washed thoroughly in distilled water and ethanol.
Precautions:	hazards in preparation and use of electrolyte are avoided by following recommended practice [7,8].